

# Mechanism of selenium pink colouration in glass

A. PAUL

*Department of Glass Technology, University of Sheffield, UK*

The mechanism of pink colouration with selenium in glass has been studied. When selenium-containing glasses are melted under reducing conditions, loss of selenium from the melt is decreased but a dark brown colour results due to the iron-selenide-oxide complex formation. Even a small amount of  $\text{CeO}_2$  in the batch\* oxidizes selenium and bleaches the pink colour; large concentrations of arsenic oxide in the batch also have the same effect. Oxidizing conditions in the melt do not produce any larger selenium loss from the melt than that with "neutral" melting conditions. On electron microscope examination, pink glasses coloured with selenium revealed spherical particles. Mie's scattering curves due to spherical selenium particles of different average sizes and size distributions have been calculated and the experimental absorption bands of pink selenium glasses have been shown to be consistent with elemental selenium particles of average diameter 50 to 250 nm with large size distributions.

## 1. Introduction

Selenium produces a pink colour which is complementary to the bluish green colour of iron in glass and is extensively used for de-colourizing commercial glasses. The shade of colour produced by selenium changes with the glass composition, furnace atmosphere and thermal history; to get optimum and reproducible effect with selenium, the batch materials and melting conditions have to be controlled very accurately. Glasses containing selenium, if melted under reducing conditions, produce a brown to black colour due to the ferric-oxide-selenide complex formation [1]. On the other hand, if selenium containing glasses are melted in oxidizing conditions, either by adding  $\text{CeO}_2$  or large excess of  $\text{As}_2\text{O}_3$  with the batch, or by keeping the furnace atmosphere oxidizing, the pink colour due to selenium is bleached due to oxidation of selenium to  $\text{SeO}_2$  or  $\text{SeO}_3$  [2]. The oxidation states and other details of selenium responsible for the pink colour in glass is not definitely known. In the present investigation attempts have been made to find the mechanism of selenium colouration in glass and the effects of  $\text{As}_2\text{O}_3$  or  $\text{CeO}_2$  addition with the batch.

## 2. Experimental

A glass of molar composition  $15\text{Na}_2\text{O}$ ,  $10\text{CaO}$ ,  $75\text{SiO}_2$  was used for this investigation. Acid washed Indian quartz (iron content less than 0.001 wt %) and Analar grades of  $\text{Na}_2\text{CO}_3$  and  $\text{CaCO}_3$  were used as batch materials. Selenium was added as elemental selenium powder with the batch. Batch materials to yield 200 g of glass were thoroughly mixed and melted in a Pt + 2% Rh crucible at  $1450^\circ\text{C}$  for 6 h in an electric furnace with air as the furnace atmosphere. During an initial 4 h of melting, the melt was stirred mechanically to increase homogeneity. The melt was cast as circular discs of 2 in. diameter and thoroughly annealed; the parallel flat surfaces were ground and polished and optical absorption spectra measured from 10 000 to 50 000  $\text{cm}^{-1}$  on a Cary-14 spectrophotometer. The glass discs were then used to estimate total selenium with X-ray fluorescence. After fluorescence measurement the glass slab was finely powdered and used for chemical estimation of minor constituents such as cerium and iron. A series of five glasses was made with different amounts of selenium; the selenium contents of these glasses were estimated chemi-

\*The batch is the raw materials mixed to produce glass after melting.

TABLE I Minor constituents of glass

Glass number	Batch composition (wt %)				Glass composition (wt %)*			
	As <sub>2</sub> O <sub>3</sub>	CeO <sub>2</sub>	Selenium	Carbon	Total iron as Fe <sub>2</sub> O <sub>3</sub>	Total arsenic as As <sub>2</sub> O <sub>3</sub>	Total cerium as CeO <sub>2</sub>	Total selenium
1	—	—	—	—	0.000 81	—	—	—
2	1.0	—	—	—	0.000 80	0.731	—	—
3	—	—	0.05	—	0.000 75	—	—	0.013 1
4	—	—	0.10	—	0.000 73	—	—	0.014 8
5	0.5	—	0.05	—	0.000 73	0.384 4	—	0.010 5
6	1.0	—	0.05	—	0.000 79	0.668 2	—	0.011 9
7	1.0	—	0.10	—	0.000 81	0.684 2	—	0.014 1
8	—	—	0.05	0.5	0.000 87	—	—	0.043 4
9	—	0.50	—	—	0.000 81	—	0.493	—
10	—	0.50	0.10	—	0.000 80	—	0.478	0.021 2
11	—	0.10	0.10	—	0.000 79	—	0.101	0.014 3
12	—	0.30	0.10	—	0.000 80	—	0.298	0.015 8
13	2.0	—	0.05	—	0.000 81	1.382	—	0.012 9

\*After chemical analysis.

cally [3], and the results used for calibration of X-ray fluorescence data which was subsequently used for estimating selenium content of all other glasses. The amount of arsenic was estimated by the Andrew's method [4], and total cerium was estimated colorimetrically with 8-hydroxy quinoline reagent [5].

### 3. Results

The estimated minor constituents of all the glasses are given in Table I. Glass 13 was only

faintly pink and glasses 10, 11 and 12 were completely colourless although all these glasses contained substantial amounts of selenium dissolved in them. Figs. 1 and 2 show the optical absorption spectra of all these glasses. Selenium-containing pink glasses undergo irreversible changes in optical absorption on heat-treatment; Fig. 3 shows the absorption spectra of glass 4 before and after heat-treatment at 600°C for 16 h. Fig. 4 shows the electron micrographs of glasses 1 and 4. In glass 4 definite spherical particles can be seen but they are absent in glass 1. The average size of the spherical particles range from 60 to 250 nm.

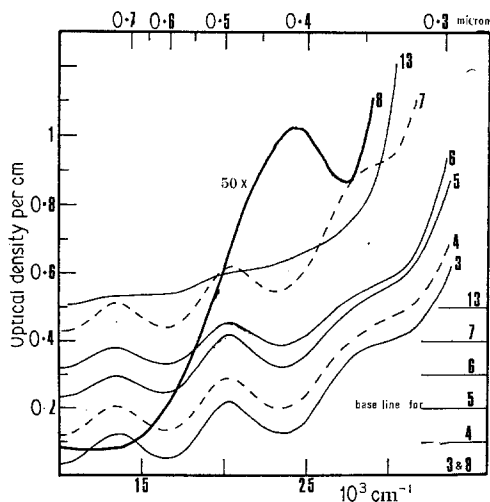


Figure 1 Optical absorption spectra of glasses from  $10 \times 10^3$  to  $30 \times 10^3$   $\text{cm}^{-1}$ .

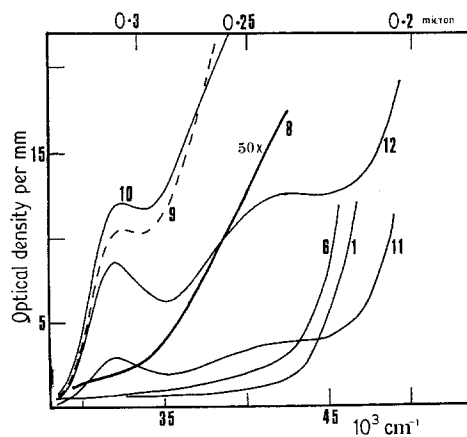


Figure 2 Optical absorption spectra of glasses from  $30 \times 10^3$  to  $50 \times 10^3$   $\text{cm}^{-1}$ .

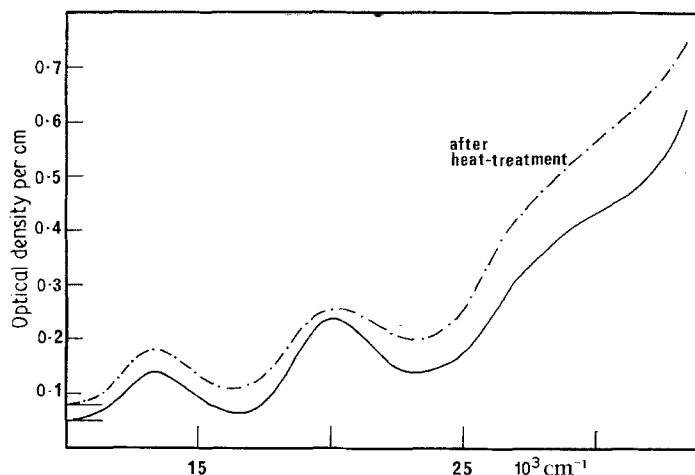


Figure 3 Optical absorption spectra of glass 4 before and after heat-treatment at 600°C for 16 h.

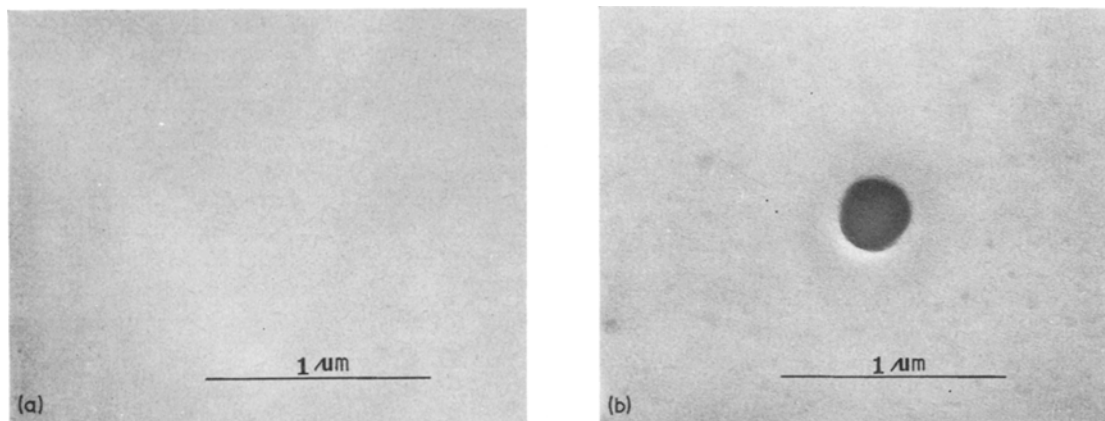


Figure 4 Replica electron micrograph of (a) glass 1 and (b) glass 4.

#### 4. Discussion

The common oxidation states of selenium are  $-2$  (selenide),  $0$  (elemental selenium),  $+4$  (selenite),  $+5$  ( $\text{Se}_2\text{O}_5$ ) and  $+6$  (selenate). In addition, the existence of  $\text{SeO}$  ( $+2$ ) has been reported in the gas phase [6]. The qualitative standard free energies of formation of different oxides of selenium, arsenic, iron and cerium are shown in Fig. 5. These values are calculated by using the room temperature heat of formation and entropy data available in the literature, and thus have a reliability of about  $\pm 10$  kcal. In Fig. 5, the cerium system lies well above the  $\text{Se}-\text{SeO}_2$  line; the mean difference being about  $33 \text{ kcal mol}^{-1}$  oxygen. This indicates a very strong oxidizing action of  $\text{CeO}_2$  on elemental selenium; or in other words  $\text{CeO}_2$  in glass will

almost quantitatively oxidize elemental selenium to higher oxidation states. Comparing the standard free energy lines for  $\text{As}_2\text{O}_3-\text{As}_2\text{O}_5$  and  $\text{Se}-\text{SeO}_2$  systems, it may be seen that the arsenic line lies just above the  $\text{Se}-\text{SeO}_2$  line; the difference (about  $5 \text{ kcal mol}^{-1}$  oxygen) is within the limits of error reported for free energy data in the literature. Thus whether or not arsenic will oxidize selenium cannot be said with certainty from this diagram; if arsenic does oxidize selenium, then for effective oxidation the arsenic/selenium ratio in the glass must be very high, for the oxidation equilibrium constant is small. However, the  $\text{FeO}-\text{Fe}_2\text{O}_3$  line lies well below the arsenic line, and indeed arsenic is well known to oxidize  $\text{FeO}$  in glass. The standard free energy data for the system  $\text{Na}_2\text{Se}-$

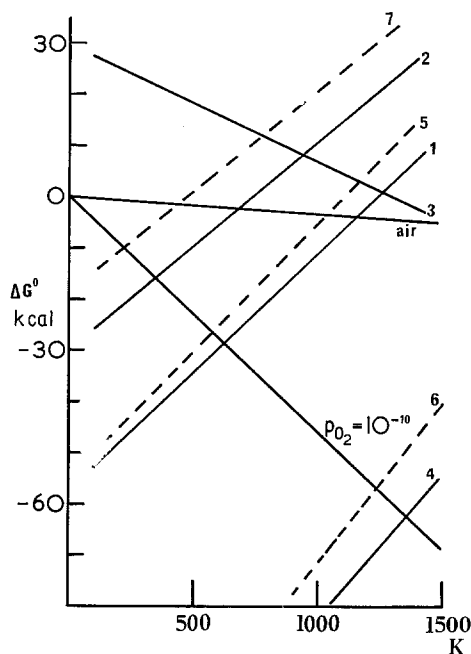


Figure 5 Extrapolated standard free energy changes (per mol oxygen) for different oxides of selenium, arsenic, iron and cerium.

- Curve 1:  $\text{Se(s)} + \text{O}_2(\text{g}) \rightleftharpoons \text{SeO}_2(\text{s})$   
 2:  $\frac{2}{3} \text{Se(s)} + \text{O}_2(\text{g}) \rightleftharpoons \frac{2}{3} \text{SeO}_3(\text{s})$   
 3:  $2 \text{Se(s)} + \text{O}_2(\text{g}) \rightleftharpoons 2 \text{SeO}(\text{g})$   
 4:  $\frac{1}{2} \text{Na}_2\text{S(s)} + \text{O}_2(\text{g}) \rightleftharpoons \frac{1}{2} \text{Na}_2\text{SO}_4(\text{s})$   
 5:  $\text{As}_2\text{O}_3(\text{s}) + \text{O}_2(\text{g}) \rightleftharpoons \text{As}_2\text{O}_5(\text{s})$   
 6:  $4 \text{FeO(s)} + \text{O}_2(\text{g}) \rightleftharpoons 2 \text{Fe}_2\text{O}_3(\text{s})$   
 7:  $2 \text{Ce}_2\text{O}_3(\text{s}) + \text{O}_2(\text{g}) \rightleftharpoons 4 \text{CeO}_2(\text{s})$

$\text{Na}_2\text{SeO}_4$  is not known. In Fig. 5 the standard free energy of the analogous system:  $\text{Na}_2\text{S}-\text{Na}_2\text{SO}_4$  is shown as line 4. Since selenium is more metallic than sulphur, it is expected that at any temperature the  $\text{Na}_2\text{Se}-\text{Na}_2\text{SeO}_4$  line will lie below that of  $\text{Na}_2\text{S}-\text{Na}_2\text{SO}_4$  line. Thus to produce  $\text{Se}^{2-}$  at  $1450^\circ\text{C}$  will require a strongly reducing condition (say  $p\text{O}_2 \leq 10^{-10}$  atm) and this, when ferric iron is present in the melt, will complex with it with the formation of the ferric-oxide-selenide chromophore producing very deep brown to black colour as shown in Fig. 2 for glass 8.

Existence of polysulphides and polyselenides in glass has been speculated in the literature [7]. However, it has become apparent in recent years that most of the absorption ascribed to polyselenides in glass is really due to traces of iron complexed with oxygen and selenide [1].

Selenite and selenate do not absorb in the

visible region. A concentrated solution of sodium selenate in water does not absorb even up to 200 nm; sodium selenite solution in water has strong absorption around 200 nm which extends to the low energy side up to about 300 nm depending upon the concentration. Under oxidizing or neutral conditions of melting, there is little probability for the formation of selenide in the melt, which, similar to sulphide, would absorb strongly in the ultraviolet region. Thus the usual pink colour of selenium in glass seems to originate from elemental selenium.

#### 4.1. Mie's theory for selenium sol in glass

The scattering of light by homogeneous sphere is described by Mie's solution of Maxwell's equations [8, 9]. These general theoretical relations cover the optical behaviour of spherical particles of any size or material. A plane electromagnetic wave incident on a homogeneous sphere induces the movement of electrons. This gives rise to radiation which may be broken down into electric and magnetic partial waves described, respectively by the different terms of the solution given by Mie in series form.

According to Beer-Lambert law, the intensity of an incident beam decreases at a distance  $l$  by the fraction  $\exp(-\gamma l)$ , where the extinction coefficient  $\gamma$  can be computed by performing the sum of the contributions of the  $n$  electric and magnetic partial waves  $a_n$  and  $b_n$ :

$$\gamma = N \frac{\lambda^2}{2\pi} \sum_n (2n+1) \text{Re}(a_n + b_n) \quad (1)$$

where:

$$a_n = \frac{\psi'_n(\beta) \psi_n(\alpha) - m \psi_n(\beta) \psi'_n(\alpha)}{\psi'_n(\beta) \xi_n(\alpha) - m \psi_n(\beta) \xi'_n(\alpha)} \quad (2)$$

$$b_n = \frac{m \psi'_n(\beta) \psi_n(\alpha) - \psi_n(\beta) \psi'_n(\alpha)}{m \psi'_n(\beta) \xi_n(\alpha) - \psi_n(\beta) \xi'_n(\alpha)} \quad (3)$$

$N$  = number of particles per  $\text{cm}^3$ ;  $\lambda_0$  = wavelength of light in vacuum;  $n_0$  = refractive index of suspending medium (glass  $\sim 1.5$ );  $\lambda = \lambda_0/n_0$  = wavelength of light in the suspending medium;  $m$  = complex refractive index of the dispersed phase relative to the suspending medium;  $\text{Re}(\dots)$  = real part of  $\dots$ ;  $r$  = particle radius;  $\alpha = 2\pi r/\lambda$  and  $\beta = m \cdot \alpha$ . This solution, involving the Riccati-Bessel functions,  $\psi_n$  and  $\xi_n$  and their derivatives  $\psi'_n$  and  $\xi'_n$  was given by Debye [10].

Let us introduce into Equation 1 the functions  $A_n$  and  $B_n$ :

$$A_n = \frac{3i(2n + 1)}{2r\alpha^2} a_n \quad (4)$$

$$B_n = \frac{3i(2n + 1)}{2r\alpha^2} b_n \quad (5)$$

$$\gamma = NV \sum_n \text{Im}(A_n + B_n) \quad (6)$$

with  $V$  = particle volume and  $\text{Im}(\dots)$  = imaginary part of  $\dots$ . Mie also writes

$$K = \frac{\gamma}{NV} = \sum_n \text{Im}(A_n + B_n). \quad (7)$$

where  $K$  is the extinction coefficient corresponding to a given volume fraction  $NV$ . The dimensions of  $K$ ,  $\gamma$ ,  $A_n$ , and  $B_n$  are  $\text{cm}^{-1}$ . The function  $K$  is very useful because it is linearly related to the measured optical density.

The number,  $n$ , of partial waves is related to the size parameter  $\alpha$ . In the case of very small particles, the sum reduces to the first electric partial wave. For larger diameters, when the size of parameter  $\alpha$  increases, more and more partial waves must be taken into account.

As is clear from the above discussion evaluation of the scattering functions of a coloured dispersed substance, such as selenium, involves the knowledge of experimental values of its complex refractive index  $m$  over a large range of wavelengths. The available data for selenium present considerable discrepancies [11-13]. However, in 1959 Koehler *et al.* [14] reported experimental values of  $m$  from measurements on carefully evaporated amorphous selenium films of various thickness, in the wavelength range 240 to 2500 nm; their results are shown in Fig. 6. These films are non-absorbing for wavelengths greater than 530 nm.

The functions  $A_n$ ,  $B_n$ , and  $K$  have been computed for a range of wavelengths 240 to 1100 nm and for various particle diameters up to 500

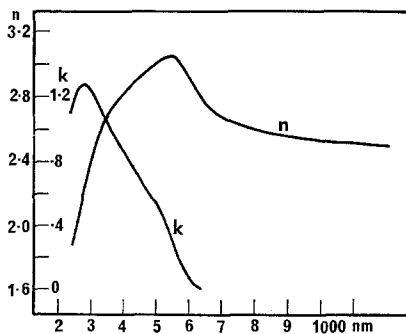


Figure 6 Complex refractive index of selenium (after [14]).

nm; some of the computed results are shown in Fig. 7. It must be pointed out that  $A_n$ ,  $B_n$  and  $K$  correspond to a volume fraction  $NV = 1$  and to a light path  $l = 1$  cm.

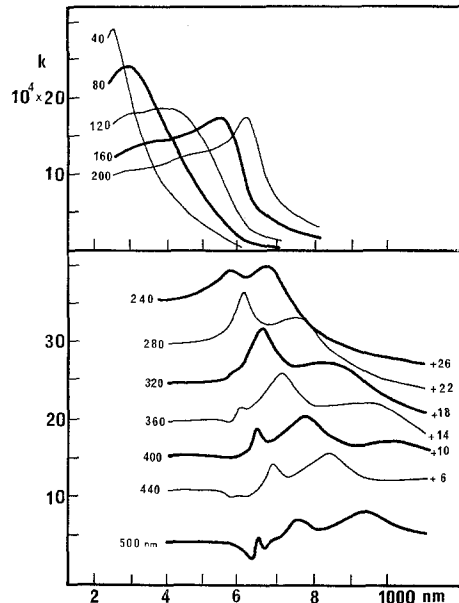


Figure 7 Extinction coefficient,  $K$ , versus wavelength for selenium particles of different sizes. (The absorption curves have been displaced vertically for clarity; the amount of displacement is indicated on the right hand side of the diagram.)

As can be seen from Fig. 7, for small particles, the extinction has a maximum for short wavelengths. With increasing diameters, the extinction maximum shifts to longer wavelengths. For diameters ranging from 40 to 220 nm, the maximum wavelength shifts from 250 to 630 nm. The presence of a second maximum can be observed from a particle diameter = 240 nm, while a third is evident above a diameter of 360 nm, and a fourth can be seen above 500 nm. Each of these maxima is situated at a shorter wavelength than the preceding one, and they all shift to longer wavelengths with increasing particle size.

The extinction curves in Fig. 7 were computed assuming an ideal monodispersity of the sols. In fact, since there is always a finite distribution of particle sizes, the effect of the degree of dispersion on the extinction coefficient was studied next. The choice of distribution function is difficult when the sols present a large heterodispersity. However, electron microscopy showed

that selenium sols in aqueous media are spherical [15, 16]. The extinction curves were calculated assuming normal size distributions with different degrees of standard deviations; some of the results are shown in Fig. 8 for particles of average diameter of 300 and 100 nm. An increase of standard deviation,  $\delta$  induces a lowering and a broadening of the extinction maxima and an increase in  $K$  values at large wavelengths. For a given standard deviation, with increasing particle size, the extinction curve deviates more and more from the ideal calculated for a monodisperse system. Thus, for large particles, the extinction curves are very sensitive to size distribution, even for small values.

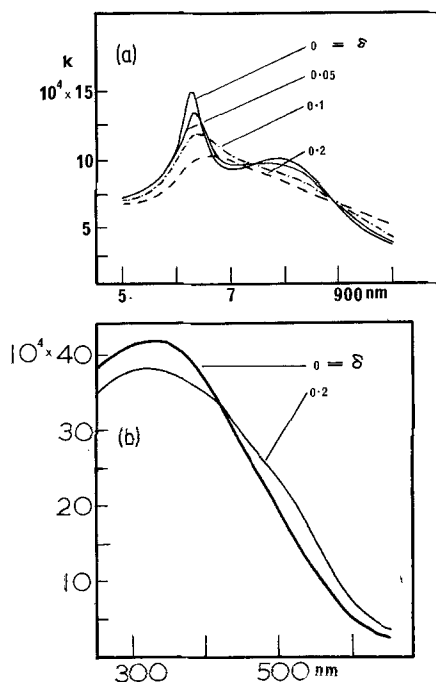


Figure 8 Influence of the size distribution on the extinction curve: average diameter (a) 300 nm, (b) 100 nm.

#### 4.2. Discussion of the present experimental results

Loss of selenium during glass melting is an age old problem of the glass industry. Batch materials of glass numbers 3, 5, 6 and 12 all contained 0.05 wt % selenium. From Table I it can be seen that 70 to 75% selenium was lost during melting from all these glasses; addition of 0.5, 1.0 and 2.0 wt %  $As_2O_3$  with the batch did not affect selenium loss to any significant extent. In glass number 13, the ratio arsenic/selenium is about 100, and the intensity of the pink colour has been con-

siderably reduced, presumably due to oxidation of selenium to  $SeO_2$ . Glass number 8 also contained 0.05 wt % selenium in the batch; this glass was melted with 0.5 wt % carbon and part of its total selenium is present as selenide. The selenium loss from this glass is much smaller (about 15%) than that from glasses 3, 5, 6 and 13 where selenium was distributed into elemental selenium and probably higher oxidation states ( $SeO_2$  and  $SeO_3$ ). Glass number 4 was melted under identical conditions with twice as much selenium in the batch as in glass number 3, but selenium retention in the final glass was no greater. This justifies the common industrial belief that only a small amount of selenium is retained in the glass, and increasing the selenium content in the batch only increases the loss without producing any stronger pink colouration. Glass numbers 4, 10, 11 and 12 all contained 0.10 wt % selenium in the batch and, in addition, glass numbers 10, 11 and 12 contained different amounts of  $CeO_2$  and were colourless, indicating all the selenium in these glasses was oxidized to  $SeO_2$  and  $SeO_3$ . It should be noted that losses of selenium from glass numbers 10, 11 and 12 are not significantly different from that in glass number 4. Indeed the vapour pressure of liquid selenium and  $SeO_2$  is comparable and very high even at lower temperatures reaching 1 atm at 690 and 350°C respectively (see Fig. 9).

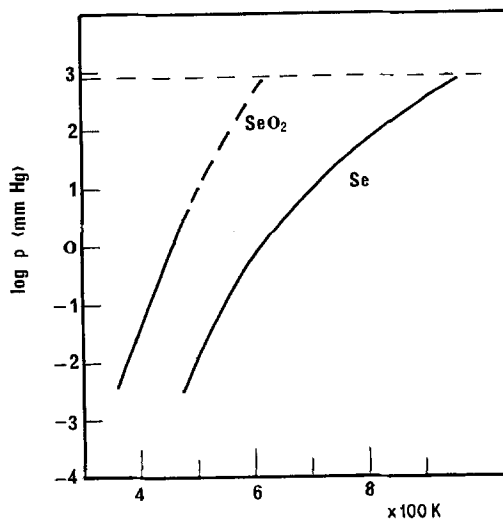


Figure 9 Vapour pressure of selenium and  $SeO_2$  at different temperatures.

In all the selenium pink glasses, three absorption bands were obtained around 690, 495 and 355 nm; although the position and half-width of

these bands changed little from glass to glass, the relative intensity changed significantly, particularly on heat-treatment (see Fig. 3). Comparing these results with the theoretical curves of Fig. 7, it can be seen that scattering bands in this region of the spectrum can arise from spherical particles of selenium of random size distribution in the range 50 to 250 nm diameter. Electron micrographs (Fig. 4) clearly show spherical particles of selenium but the volume fraction of selenium sol was so small that no quantitative measurement of their size distribution was possible.

In Fig. 3 the effect of heat-treatment appears to be an overall increase of optical density, whereas one would usually expect that upon heat-treatment the mean particle size and distribution of particle sizes would change, resulting in a shift of the maxima in the absorption spectrum. However, it is clear from Fig. 7 that the observed three absorption maxima around 690, 495 and 355 nm cannot occur for any monodisperse selenium sol in glass; selenium particles having a diameter less than 100 nm cannot produce absorption bands above 300 nm. It seems probable that upon heat-treatment, these smaller particles (which are always present in glass) coagulate with the formation of larger particles (say about 200 to 250 nm) and thus the overall absorption at lower energy increases. Since the selenium concentration in these glasses

is very small ( $\sim 0.015$  wt %), probably growth into even larger particles will involve diffusion of selenium atoms over a very large distance, which is prohibitive in the present experimental conditions.

## References

1. A. PAUL, *Phys. Chem. Glasses* **14** (1973) 96.
2. A. PONS and F. PONS, *Verres Refract.* **23** (1969) 312.
3. M. BLANKLEY, BIGRA Report No. 131 (1970).
4. A. PAUL, *Glass Technology* **6** (1965) 22.
5. P. RUDD, Ph.D. Thesis (1974), Sheffield University; F. VERNON, *J. Inorg. Nucl. Chem.* **32** (1970) 1005.
6. V. PIACENTE, L. MALASPINA and G. BARDI, *Rev. Int. Hautes Temp. Refract.* **6** (1969) 25.
7. W. A. WEYL, "Coloured Glasses" (Society of Glass Technology, Sheffield, 1959) p. 304.
8. G. MIE, *Ann. Physik.* **25** (1908) 377.
9. H. C. VAN DEHULST, "Light Scattering by small particles" (Wiley, New York, 1957).
10. P. DEBYE, *Ann. Physik.* **30** (1909) 59.
11. K. FOERSTERLING, *ibid* **43** (1914) 1227.
12. R. WOOD, *Phil. Mag.* **3** (1902) 607.
13. W. MEIER, *Ann. Physik.* **31** (1910) 1017.
14. W. F. KOEHLER, F. K. ODENCRANTZ and W. C. WHITE, *J. Opt. Soc. Amer.* **49** (1959) 109.
15. A. WATILLON and A. M. JOSEPH-PETIT, Proceedings of the International Congress on Surface activity, 3rd Cologne **A145** (1960).
16. *Idem*, Meeting of the American Chemical Society, Symposium on Coagulation and Coagulant Aids, Los Angeles (1963).

Received 29 July and accepted 11 September 1974.